Research Report

2007-28

Simulation of a Salient Pole Synchronous Machine with Both Field Pole and Stator Core Saturation

T.A. Lipo, T. Komatsu*, K. Shinohara*

Universityo f Wisconsin
MadisonW I, U.S.A.

*KagoshimUa niversity
KagkoshimaJ apan

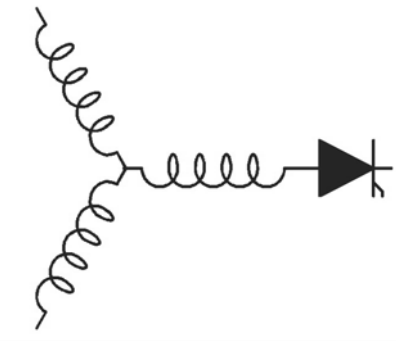

Wisconsin
Electric
Machines &
Power
Electronics
Consortium

University of Wisconsin-Madison
College of Engineering
Wisconsin Power Electronics Research Center
2559D Engineering Hall
1415 Engineering Drive
Madison WI 53706-1691

Simulation of a Salient Pole Synchronous Machine with Both Field Pole and Stator Core Saturation

T.A Lipo
University of Wisconsin
Madison WI, U.S.A.

T. Komatsu
Kagoshima University
Kagkoshima Japan

K. Shinohara
Kagoshima University
Kagkoshima Japan

Abstract - **Saturation effects in salient pole synchronous machines are generally modelled by assuming that the saturation effect is primarily limited to the field pole. However, saturation of the stator teeth and core can also become saturated such as when operating as a generator with a leading power factor load. This paper addresses the modeling and simulation of simultaneous saturation of both the stator and rotor taking into account the correct components of flux linkage which contribute to these effects. Suitable saturation curves are computed using finite element methods. Simulation results are shown using the new saturation model.**

I. Introduction

Saturation effects in salient pole synchronous machines are typically modelled by assuming that the saturation effect is primarily limited to the field pole and the effect is, hence, a function of the field flux linkages. However, situations occur in which saturation of the stator teeth and core also become saturated such as operation as a generator with a leading power factor load. The saturation effect of the stator cannot be simply lumped with the field pole saturation since stator core saturation is the vector sum of *d*– and *q*–axis stator flux linkages while the field pole is essentially dependant only on *d*–axis flux linkage components. Hence, depending upon load, saturation of a synchronous machine may have either stator saturation, field pole saturation or simultaneous saturation of both components. This paper addresses means for modeling and simulation of simultaneous saturation of both the stator and rotor taking into account the correct components of flux linkage which contribute to these effects. Suitable saturation curves are computed using finite element methods. Typical simulation results of the improved model are shown.

II. d-q Representation of a Synchronous Machine

Park's model of a salient-pole synchronous machine, represented in the rotor reference frame, is shown in Figure 1. The quantities r_s, r_{dr} r_{qr} and r_{fr} correspond to the stator, *d*–axis rotor amortisseur, *q*–axis amortisseur and field winding resistance all referred to the stator by the appropriate turns ratio. The quantities L_{md} and L_{mq} are the *d*– and *q*– axes magnetizing inductances respectively. In Figure 1 the stator leakage inductance typically expressed a L_{ls} has been separated into two portions namely L_{les} and L_{lcs} to denote the leakage inductances which correspond to the end winding and the core portions of the leakage flux linkages respectively. The two portions of the stator leakage inductances have been separated since saturation of the stator core only involves that portion of the stator leakage flux which passes through the stator core.

The equations corresponding to the circuit of Figure 1 are,

$$v_{qs} = r_s i_{qs} + \frac{d\lambda_{qs}}{dt} + \omega_r \lambda_{ds} . \tag{1}$$

$$v_{ds} = r_s i_{ds} + \frac{d\lambda_{ds}}{dt} - \omega_r \lambda_{qs} \tag{2}$$

$$v_{qr} = r_{qr} i_{qr} + \frac{d\lambda_{qr}}{dt} \tag{3}$$

$$v_{dr} = r_{dr} i_{dr} + \frac{d\lambda_{dr}}{dt} \tag{4}$$

$$v_{fr} = r_{fr} i_{fr} + \frac{d\lambda_{fr}}{dt} \tag{5}$$

For purposes of simulation Eq. 5 is usually manipulated to the form

$$e_x = \omega_b L_{md} i_{fr} + \frac{\omega_b L_{md}}{r_{fr}} \frac{d\lambda_{fr}}{dt} \tag{6}$$

where $e_x = \omega_b (L_{md} / r_{fr}) v_{fr}$ and ω_b is a selected base frequency. The amortisseur voltages v_{qr} and v_{dr} are zero except for special cases.

The flux linkages in Eqs. 1-5 are defined by referring to Figure 2. They are,

$$\lambda_{qs} = L_{les} i_{qs} + \lambda_{qcs} \tag{7}$$

$$\lambda_{ds} = L_{les} i_{ds} + \lambda_{dcs} \tag{8}$$

$$\lambda_{qr} = L_{lqr} i_{qr} + \lambda_{mq} \tag{9}$$

$$\lambda_{dr} = L_{ldr} i_{dr} + \lambda_{md} \tag{10}$$

$$\lambda_{fr} = L_{lfr} i_{fr} + \lambda_{md} \tag{11}$$

and

$$\lambda_{mq} = L_{mq}(i_{qs} + i_{qr}) \tag{12}$$

$$\lambda_{md} = L_{md}(i_{ds} + i_{dr} + i_{fr}) \tag{13}$$

$$\lambda_{qcs} = L_{lcs} i_{qs} + \lambda_{mq} \tag{14}$$

$$\lambda_{dcs} = L_{lcs} i_{ds} + \lambda_{md} \tag{15}$$

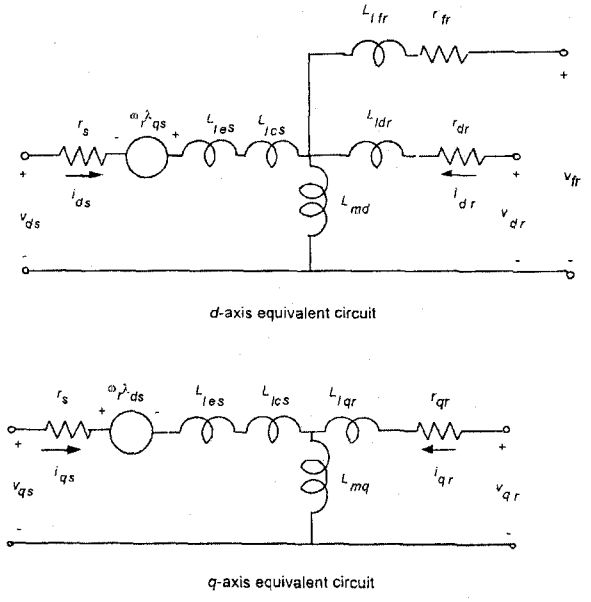

Figure 1 *d-q* axis equivalent circuit of a salient pole synchronous machine where the stator leakage inductance has been separated into saturable (core) and non-saturable (end winding) portions.

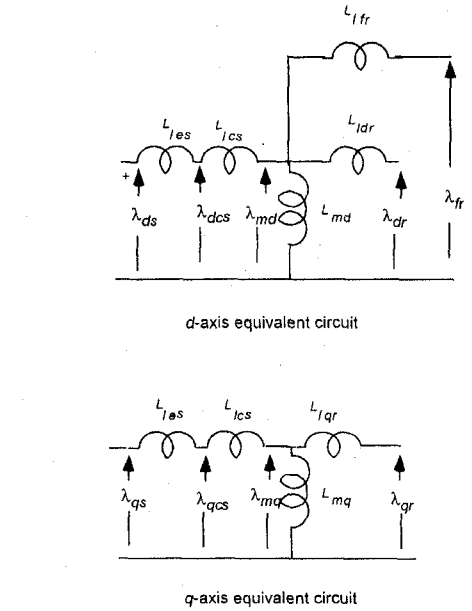

Figure 2 Flux linkages used as state variables.

The electromechanical torque produced by the machine is typically expressed as [1]

$$T_e = \left(\frac{3}{2}\right)\left(\frac{P}{2}\right)(\lambda_{ds} i_{qs} - \lambda_{qs} i_{ds}) \tag{16}$$

Finally, since the machine is generally tied to an external load/prime mover, in its simplest form the equation which describes coupling between the electrical and mechanical system can be written as

$$T_e - T_{load} = \left(\frac{2}{P}\right) J \frac{d\omega_r}{dt} \tag{17}$$

where T_{load} is the load torque (negative if the "load" corresponds to a prime mover torque) and J is combined inertia of machine and load.

II. Simulation of a Synchronous Machine Using Flux Linkages as Variables

Since the differential equations of the machines, Eqs. (1)-(5), contain mixed variables either flux linkages or currents could be eliminated from the differential equations by means of the algebraic relations, Eqs. (7)–(15)(15). Modelling of saturation is best achieved by retaining flux linkages as the state variables. The current can be solved in terms of the flux linkages as,

$$i_{qs} = \frac{\lambda_{qs} - \lambda_{qcs}}{L_{les}} \tag{18}$$

$$i_{ds} = \frac{\lambda_{ds} - \lambda_{dcs}}{L_{les}} \tag{19}$$

$$i_{qr} = \frac{\lambda_{qr} - \lambda_{mq}}{L_{lqr}} \tag{20}$$

$$i_{dr} = \frac{\lambda_{dr} - \lambda_{md}}{L_{ldr}} \tag{21}$$

$$i_{fr} = \frac{\lambda_{fr} - \lambda_{md}}{L_{lfr}} \tag{22}$$

Eliminating λ_{md} and λ_{mq} from Eqs. (18)–(20) using Eq. (14) and (15) an substituting the result into Eqs. (20)–(22),

$$i_{qr} = \lambda_{qr} + \frac{L_{lcs}}{L_{les}}\lambda_{qs} - \frac{L_{ls}}{L_{les}}\lambda_{qcs} \tag{23}$$

$$i_{dr} = \lambda_{dr} + \frac{L_{lcs}}{L_{les}}\lambda_{ds} - \frac{L_{ls}}{L_{les}}\lambda_{dcs} \tag{24}$$

$$i_{fr} = \lambda_{fr} + \frac{L_{lcs}}{L_{les}}\lambda_{ds} - \frac{L_{ls}}{L_{les}}\lambda_{dcs} \tag{25}$$

where

$$L_{ls} = L_{lcs} + L_{les} \tag{26}$$

The internal stator core flux linkages λ_{dcs} and λ_{qcs} can now be written in terms of the total stator and rotor flux linkages as

$$\lambda_{dcs} = \frac{L_{les}}{L_{ls}}\left(\frac{L_{lcs}}{L_{les}} + \frac{L_{md}^*}{L_{ls}}\right)\lambda_{ds} + \frac{L_{les}}{L_{ls}}\left(\frac{L_{md}^*}{L_{ldr}}\right)\lambda_{dr} + \frac{L_{es}}{L_{ls}}\left(\frac{L_{md}^*}{L_{lfr}}\right)\lambda_{fr} \tag{27}$$

$$\lambda_{qcs} = \frac{L_{les}}{L_{ls}}\left(\frac{L_{lcs}}{L_{les}} + \frac{L_{mq}^*}{L_{ls}}\right)\lambda_{qs} + \frac{L_{les}}{L_{ls}}\left(\frac{L_{mq}^*}{L_{lqr}}\right)\lambda_{qr} \tag{28}$$

where

$$L_{md}^* = \frac{1}{\frac{1}{L_{md}} + \frac{1}{L_{ls}} + \frac{1}{L_{ldr}} + \frac{1}{L_{lfr}}} \tag{29}$$

$$L_{mq}^* = \frac{1}{\frac{1}{L_{mq}} + \frac{1}{L_{ls}} + \frac{1}{L_{lqr}}} \tag{30}$$

These results can be inserted into the differential equations described by the circuit of Figure 1. Upon solving for the time derivative terms and integrating, the result is,

$$\lambda_{qs} = \int\left[v_{qs} + \frac{r_s}{L_{les}}(\lambda_{qcs} - \lambda_{qs}) - \omega_r\lambda_{ds}\right]dt \tag{31}$$

$$\lambda_{ds} = \int\left[v_{ds} + \frac{r_s}{L_{les}}(\lambda_{dcs} - \lambda_{ds}) + \omega_r\lambda_{qs}\right]dt \tag{32}$$

$$\lambda_{qr} = \int\left\{v_{qr} + \frac{r_{qr}}{L_{lqr}}\left[\frac{L_{ls}}{L_{lcs}}\lambda_{qcs} - \left(\lambda_{qr} + \left(\frac{L_{lcs}}{L_{les}}\right)\lambda_{qs}\right)\right]\right\}dt \tag{33}$$

$$\lambda_{dr} = \int\left\{v_{dr} + \frac{r_{dr}}{L_{ldr}}\left[\frac{L_{ls}}{L_{lcs}}\lambda_{dcs} - \left(\lambda_{dr} + \left(\frac{L_{lcs}}{L_{les}}\right)\lambda_{ds}\right)\right]\right\}dt \tag{34}$$

$$\lambda_{fr} = \int\frac{r_{fr}}{\omega_b L_{md}}\left\{e_x + \omega_b\frac{L_{md}}{L_{lfr}}\left[\frac{L_{ls}}{L_{lcs}}\lambda_{dcs} - \left(\lambda_{fr} + \left(\frac{L_{lcs}}{L_{les}}\right)\lambda_{ds}\right)\right]\right\}dt \tag{35}$$

$$\omega_r = \left(\frac{P}{2}\right)\left(\frac{1}{J}\right)\int(T_e - T_{load})dt \tag{36}$$

The flow of signals for simulation of a salient pole synchronous machine is shown in Figure 3.

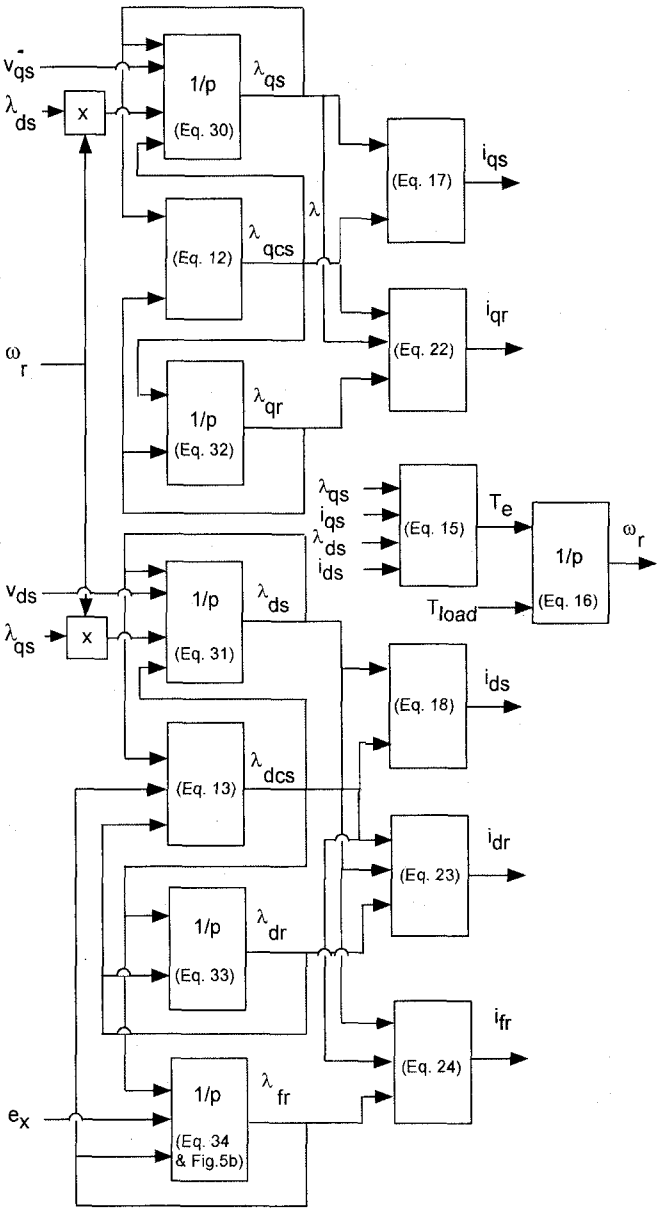

Figure 3 Signal flow diagram for a salient pole synchronous machine.

III. Modeling of Saturation

In many cases the saturation of the stator teeth for field pole dominate in which case saturation can be taken into account accurately by expressing the air gap flux linkage as a non-linear function of the air gap MMF. While the air gap MMF is difficult to determine under a loaded condition, the required relationship can be established of the motor is operated under an open circuit in which case the MMF is clearly proportional only to field current since the stator current is, in this case, zero. If the open circuit voltage is plotted versus the field current the saturation curve of Figure 4(a) can be established. The slope of a line drawn from the origin to a point on the straight line (unsaturated) portion of the curve is equal to the stator *d*–axis mutual reactance. If the abscissa of Figure 4(a) is

multiplied by the d–axis mutual reactance and the ordinate by $1/\omega_r$, the normalized curve of Figure 4(b) results in which the abscissa remains proportional to MMF while having the units of webers. The slope of the unsaturated portion of the curve is now clearly unity. The difference between the saturated and unsaturated values of air gap flux linkage can be defined as $\Delta\lambda_{ag}$ as illustrated on the figure.

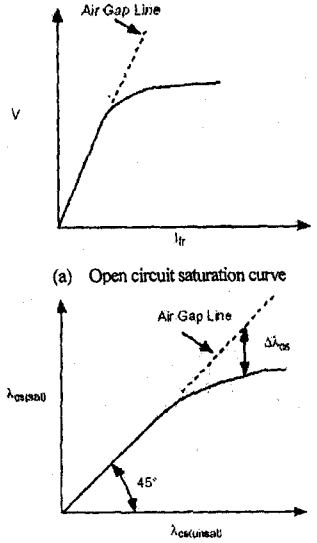

Figure 4 (a) Open circuit saturation curve and (b) derived curve.

In general, the same approach can be used to model the saturation of the stator core. In this case the core flux linkage is noted as λ_{cs} and the deviation from the unsaturated value as $\Delta\lambda_{cs}$. The value of $\Delta\lambda_{cs}$ can now be plotted as a function of the unsaturated value of stator core flux linkages $\lambda_{cs(unsat)}$. Since saturation does not result in a phase shift in the fundamental component of flux linkages and only decreases the amplitude, both the *d*– and *q*– components of saturated core flux should be decreased by the same value. Thus,

$$\Delta\lambda_{dcs} = \frac{\lambda_{dcs(unsat)}}{\lambda_{cs(unsat)}}\Delta\lambda_{cs} \tag{37}$$

$$\Delta\lambda_{qcs} = \frac{\lambda_{qcs(unsat)}}{\lambda_{cs(unsat)}}\Delta\lambda_{cs} \tag{38}$$

where

$$\lambda_{cs(unsat)} = \sqrt{(\lambda_{dcs(unsat)})^2 + (\lambda_{dcs(unsat)})^2} \tag{39}$$

and

$$\Delta\lambda_{cs} = f(\lambda_{cs(unsat)}) \tag{40}$$

represents the saturation curve.

Saturation of the *q*–axis can now be incorporated if Eqs. (7) and (9) are modified to the form,

$$\lambda_{qs} = L_{lcs}i_{qs} + \lambda_{qcs(sat)} \tag{41}$$

$$= L_{lcs}i_{qs} + \lambda_{qcs(unsat)} - \Delta\lambda_{qcs} \tag{42}$$

When combined with Eq. (12), the *q*–axis portion of the unsaturated value of flux linkage is

$$\lambda_{qcs(unsat)} = L_{cq}^*\left[\left(\left(\frac{L_{lcs}}{L_{les}}\right)\frac{1}{L_{mq}} + \frac{1}{L_{les}} + \frac{L_{lcs}}{L_{les}}\frac{1}{L_{lqr}}\right)\lambda_{qs}\right] + \frac{\lambda_{qr}}{L_{lqr}} + \frac{\Delta\lambda_{qcs}}{L_{mq}}\Bigg] \tag{43}$$

Similarly

$$\lambda_{dcs(unsat)} = L_{cd}^*\left[\left(\left(\frac{L_{lcs}}{L_{les}}\right)\frac{1}{L_{md}} + \frac{1}{L_{les}} + \frac{L_{lcs}}{L_{les}}\frac{1}{L_{ldr}} + \frac{L_{lcs}}{L_{les}}\frac{1}{L_{lfr}}\right)\lambda_{ds} + \frac{\lambda_{dr}}{L_{ldr}} + \frac{\lambda_{fr}}{L_{lfr}} + \frac{\Delta\lambda_{dcs}}{L_{md}}\right] \tag{44}$$

where, for convenience, the following quantities have been defined,

$$L_{cq}^* = \frac{1}{\frac{1}{L_{mq}} + \frac{L_{lcs}}{L_{les}}\frac{1}{L_{mq}} + \frac{1}{L_{les}} + \frac{L_{lcs}}{L_{les}}\frac{1}{L_{lqr}}} \tag{45}$$

$$L_{cd}^* = \frac{1}{\frac{1}{L_{md}} + \frac{L_{lcs}}{L_{les}}\frac{1}{L_{md}} + \frac{1}{L_{les}} + \frac{L_{lcs}}{L_{les}}\frac{1}{L_{ldr}} + \frac{L_{lcs}}{L_{les}}\frac{1}{L_{lfr}}} \tag{46}$$

Saturation of the field pole can be implemented in the usual fashion. Specifically, the equation for field flux linkages, Eq. (11), with the help of Eq. (13), be modified to the form

$$L_{md}i_{fr} = \frac{L_{md}}{L_{md}+L_{lfr}}\lambda_{fr} - \frac{L_{md}^2}{L_{lfr}+L_{md}}(i_{ds}+i_{dr}) \tag{47}$$

When the field pole is saturated extra field current must be added to account for saturation. Eq. (47) becomes

$$(L_{md}i_{fr})_{sat} = \frac{L_{md}}{L_{md}+L_{lfr}}\lambda_{fr} + \Delta(L_{md}i_{fr}) - \frac{L_{md}^2}{L_{lfr}+L_{md}}(i_{ds}+i_{dr}) \tag{48}$$

The proper value of $\Delta(L_{md}i_{fr})$ is typically discerned from the open circuit saturation curve, Fig. 4(a). Signal flow models of the two saturation effects are implemented in Figure 5.

IV. Finite Element Analysis

When saturation of the magnetic circuit of a synchronous machine is lumped in terms of a single saturation curve, the information need to determine the degree of saturation can be

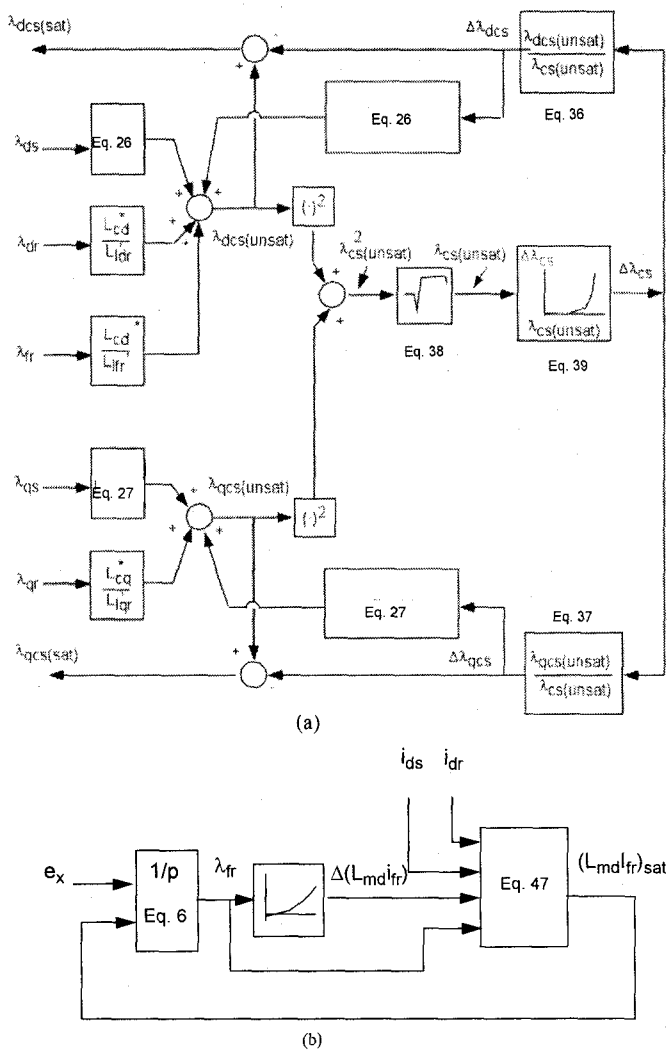

Figure 5 Flow diagram for simulation of (a) stator core saturation and (b) field pole saturation.

discerned from the open circuit saturation curve as described in Section III. However, since the two saturation effects under consideration exist in series for the no load test, the individual saturation curves can not be determined without an arbitrary assumption concerning the split of the MMF drops across the two iron portions. A preferable alternative is to employ finite element analysis, assuming that the basic geometry of the machine is known. Figure 6 shows the FEM model used to verify the solution. The saturation curves can be determined by systematically first setting the stator iron permeability to infinity and then setting the rotor iron permeability to infinity. The results of the calculations are shown in Figure 7. The two saturation curves deduced from Figure Figure 7 is shown in Figure 8.

V. MATLAB/SIMULINK RESULTS

The simulation flow diagrams are readily implemented in Matlab/Simulink or similar computer programs. Figure 9 shows traces for a line start using the flow diagrams of Figs. 3

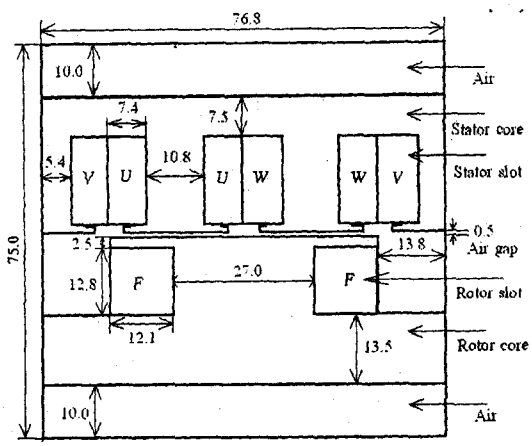

Figure 6 Dimensions of one pole of synchronous machine studied using finite elements.

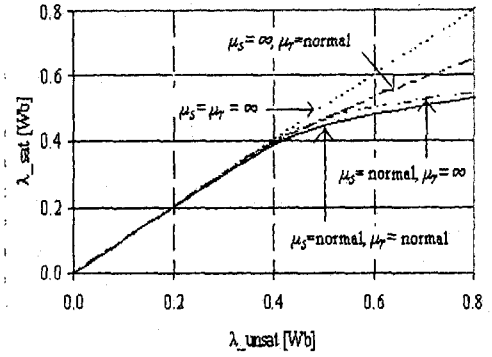

Figure 7 Saturation curves produced by finite elements.

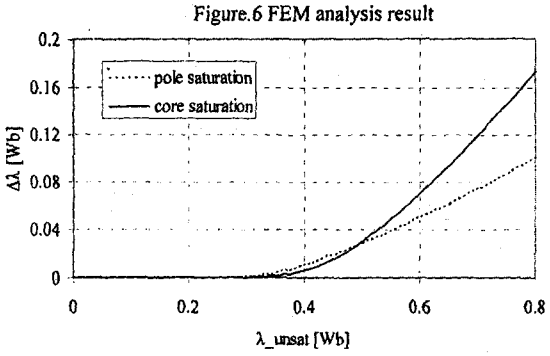

Figure 8 Core and Pole saturation curves.

and 5. In, general the time for acceleration increases by about 20% compared to an unsaturated model and is less damped when the machine pulls into synchronism.

VI. CONCLUSION

This paper has presented a method for modelling both stator core and field pole saturation. Simulation studies indicate that the overall behavior is less damped than with simple field pole saturation. Use of this new model should

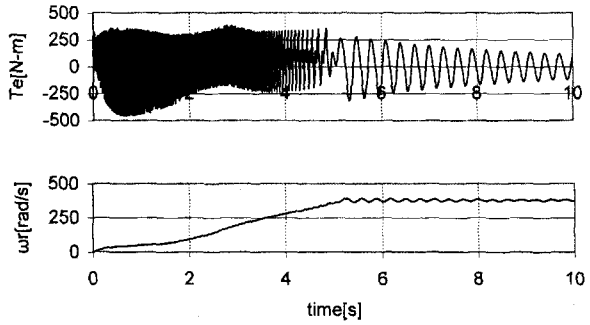

Figure 9 Torque and Speed during acceleration from rest.

prove particularly beneficial in motor drive applications in which large torque demands (q–axis stator current) are made on the machine resulting in heavy stator core saturation even when accompanied by a relatively modest value of field current.

REFERENCES

[1] D.W. Novotny and T.A. Lipo, "Dynamics and Vector Control of AC Drives", (book) Oxford Press, 1996.